Texture Classification and Visualization of Time Series of Gait Dynamics in Patients With Neuro-Degenerative Diseases

Tuan D. Pham, *Senior Member, IEEE*

***Abstract*— The analysis of gait dynamics is helpful for predicting and improving the quality of life, morbidity, and mortality in neuro-degenerative patients. Feature extraction of physiological time series and classification between gait patterns of healthy control subjects and patients are usually carried out on the basis of 1-D signal analysis. The proposed approach presented in this paper departs itself from conventional methods for gait analysis by transforming time series into images, of which texture features can be extracted from methods of texture analysis. Here, the fuzzy recurrence plot algorithm is applied to transform gait time series into texture images, which can be visualized to gain insight into disease patterns. Several texture features are then extracted from fuzzy recurrence plots using the gray-level co-occurrence matrix for pattern analysis and machine classification to differentiate healthy control subjects from patients with Parkinson's disease, Huntington's disease, and amyotrophic lateral sclerosis. Experimental results using only the right stride-intervals of the four groups show the effectiveness of the application of the proposed approach.**

***Index Terms*— Gait dynamics, Parkinson's disease, Huntington's disease, amyotrophic lateral sclerosis, time series, fuzzy recurrence plots, texture analysis, pattern classification.**

I. Introduction

IT IS known that neuro-degenerative diseases often affect gait and mobility. Gait abnormality is a deviation from normal walking, and the observation of the pattern of a patient's walk is thought to be the most important part of the neurological assessment. Normal gait depends on the integration of strength, sensation and coordination. It is how a person walks can reveal disorder in the nervous and musculoskeletal systems [1]. Therefore in order to gain better understanding of the pathophysiology of these disorders, and to enhance the ability for evaluating responses to therapeutic interventions, it is important to accurately quantify gait dynamics.

Evidence of different behaviors in healthy control subjects and patients with neuro-degenerative disease has been found in the fluctuations in time series of stride-to-stride measures of footfall contact times. These altered stride intervals indicate changes in neurological functions associated with aging and certain disease staging, as suggested in [2] with the use of the power law to derive a scaling exponent for elderly, young, and Huntington's disease (HD), which is disorder that causes the progressive degeneration of of nerve cells in the brain. The scaling exponent was found to be higher in young subjects than elderly subjects, and higher in healthy control (HC) group than the patients with HD. Altered gait rhythm was found in patients with amyotrophic lateral sclerosis (ALS), which is a neural disorder caused by the loss of motoneurons, and evidence of altered stride dynamics was also found in advanced ALS, HD, and Parkinson's disease (PD) [3], which is a progressive degeneration of the nervous system that affects the motor system or movement.

Based on the findings reported in [2] and [3] and the available associated gait datasets, several studies have been attempted to extract new features of the time series of the gait rhythm for pattern analysis and classification of HC, PD, HD, and ALS subjects. Wu and Krishnan [4] applied the Parzen window method to estimate the probability density function of the stride intervals and its subphases, which are the swing and stance intervals, and the signal turn counts of the time series to characterize and classify HC and PD groups using the least squares support vector machines. In a similar study, Khorasani and Daliri [5] applied the hidden Markov models for the classifying the time series of the right stride interval of HC and PD subjects. Zeng and Wang [6] applied the theory of dynamic learning to classify HC, PD, HD, and ALS subjects using features extracted from the left and right swing intervals and the left and right stance intervals, where the work in [7] used a different database for the classification of HC and PD subjects based on the theory of dynamic learning. Most recently, Ren *et al.* [9] studied the gait fluctuations of HC, PD, HD, and ALS using the empirical mode decomposition to extract two parameters for characterizing the four groups, and used several classifiers trained with these parameters to carry out the classification of the four groups.

The work presented in this paper attempts to extract texture features from time series of gait dynamics in HC, PD, HD, and ALS by transforming the one-dimensional signals (time series) into two-dimensional texture objects (images) using the method of fuzzy recurrence plots (FRPs) [10]. The FRPs not only can be useful as a visualization tool but their textural information can be readily extracted by texture analysis methods for pattern analysis and classification. Here, the gray-level co-occurrence matrix (GLCM) method is utilized to obtain

Manuscript received April 27, 2017; accepted July 24, 2017. Date of publication July 27, 2017; date of current version January 8, 2018.

The author is with the Department of Biomedical Engineering, Linköping University, 581 83 Linköping, Sweden (e-mail: tuan.pham@liu.se).

Digital Object Identifier 10.1109/TNSRE.2017.2732448

various texture features of the FRPs because the similarity in the underlying formulations of FRP and GLCM methods (both methods work on capturing information about recurrences of variables in space). State-of-the-art machine learning method trained with the GLCM-based texture features is applied for differentiating HC subjects from the three groups of patients with neuro-degenerative diseases.

The rest of this paper is organized as follows. Section II introduces the concept of the fuzzy recurrence plots. Section III briefly outlines the construction of a gray-level co-occurrence matrix, which can be utilized to extract several texture features from the fuzzy recurrence plots. Section IV describes the database to be for testing and comparing the performance of the proposed approach with other methods mentioned earlier. Section V includes experimental results, comparisons, and discussion. Finally, Section VI is the conclusion of the finding and suggestions for further research.

II. Fuzzy Recurrence Plots

The mathematical development of fuzzy recurrence plots has been originally introduced in [10], and will be described herein for the purpose of self-contained information about the algorithm for transforming a time series into a textural image.

A recurrence plot (RP) is a square binary matrix or image, in which each pixel indicates the recurrence of a corresponding state of a dynamical system. In mathematical terms, let $X = \{x\}$ be a set of phase-space states, in which x_i is the i-th state of a dynamical system in m embedding dimensions. An RP is an $N \times N$ image in which a pixel $(i, j) \in \{0, 1\}$, $i = 1, \ldots, N$, $j = 1, \ldots, N$, is 0 if x_i and x_j are considered to be closed to each other [11]. A symmetrical RP is defined as [12]:

$$RP(i, j) = H(\epsilon - \|x_i - x_j\|), \tag{1}$$

where $RP(i, j)$ is an element (i, j) of the recurrence image RP, ϵ is a similarity threshold, and $H(\cdot)$ is the Heaviside step function or the unit step function that yields either 0 or 1 if $(\epsilon - \|x_i - x_j\|) < 0$ or otherwise, respectively.

As an RP is a binary image, its textural information is therefore limited. The concept of a fuzzy recurrence plot (FRP) [10] allows to construct the recurrence image that takes values in [0, 1] to enhance the texture and to relax the selection of the critical threshold parameter ϵ required by the RP analysis. Let $V = \{v\}$ be the set of fuzzy clusters of the states. A fuzzy (binary) relation R from X to V is a fuzzy subset of $X \times V$ characterized by a fuzzy membership function $\mu \in [0, 1]$. This fuzzy membership grade expresses the strength of relation of each pair (x, v) in R that has the following properties [13]:

1) Reflexivity: $\mu(x, x) = 1$, $\forall x \in X$.
2) Symmetry: $\mu(x, v) = \mu(v, x)$, $\forall x \in X, \forall v \in V$.
3) Transitivity: $\mu(x, z) = \vee_v[\mu(x, v) \wedge \mu(v, z)]$, $\forall x \in X$, $\forall z \in Z$, which is called the max-min composition, where the symbols $\vee$ and $\wedge$ stand for max and min, respectively.

The fuzzy c-means (FCM) algorithm [14] can be applied to obtain the fuzzy clusters of the phase-space states to determine the closeness between the states and their fuzzy cluster centers, based on which the inference of the similarity between the pairs of the states can be made using the max-min composition of a fuzzy relation. Let $\{x_1, x_2, \ldots, x_N\}$ be a set of phase-space states of the system, the FCM algorithm tries to minimize the following fuzzy objective function using a numerical solution [14]:

$$J(U, Z) = \sum_{i=1}^{N} \sum_{j=1}^{c} (\mu_{ij})^w \, [d(x_i, z_j)]^2, \tag{2}$$

where c is the number of clusters, $1 < c < N$, $w \in [1, \infty)$ is the fuzzy weighting exponent, $U = [\mu_{ij}]$, $i = 1, \ldots, N$, $j = 1, \ldots, c$, is the matrix of the fuzzy c-partition, $Z = (z_1, z_2, \ldots, z_c)$ is the vector of cluster centers, z_j is the center of cluster j, and $d(x_i, z_j)$ is any inner-product induced norm metric.

The fuzzy objective function expressed in Equation (2) is subject to

$$\sum_{j=1}^{c} \mu_{ij} = 1, \quad i = 1, \ldots, N \tag{3}$$

where $\mu_{ij} \in [0, 1], i = 1, \ldots, N, \; j = 1, \ldots, c$.

In order to optimally determine U and Z, a numerical solution to the minimization of the objective function $J(U, Z)$ is by an iterative process of updating U and Z until some convergence is reached. The fuzzy membership grades and cluster centers of the FCM can be updated as follows [14]:

$$\mu_{ij} = \frac{1}{\sum_{j=1}^{c} \left[\frac{d(x_i, z_k)}{d(x_i, z_j)} \right]^{2/(w-1)}}, \quad 1 \le k \le c; \tag{4}$$

$$z_j = \frac{\sum_{i=1}^{N} (\mu_{ij})^w \, x_i}{\sum_{i=1}^{N} (\mu_{ij})^w}, \quad \forall j. \tag{5}$$

The updating process is stopped if $\|U^t - U^{t+1}\| \le \kappa$, where t is the t-th time step, and κ is a small positive real number that indicates the minimum level of improvement.

III. Texture Analysis of Fuzzy Recurrence Plots

The gray-level co-occurrence matrix (GLCM) [15] constructs a matrix that reflects the co-occurrences of all pairs of pixels that are separated from a certain distance d. An element of a GLCM can be mathematically expressed as [16]

$$C_d(k, l) = \sum_i \sum_j \sum_\theta \delta[k, g(i, j)] \delta[l, g((i, j) + d\theta)], \tag{6}$$

where k, l are gray values, $g(i, j)$ is the gray value of pixel (i, j), $g(i, j) + d\theta$ is the gray value of another pixel that is separated by a distance d from pixel (i, j) and at an orientation defined by unit vector θ, $\delta(a, b)$ is the Kronecker delta that is 1 if $a = b$, and 0 if $a \neq b$.

The joint probability density of the GLCM, denoted as $p(i, j)$, can be determined by dividing each element of the GLCM by the total number of pairs of pixels that co-occur, recorded in the GLCM. Using $p(i, j)$ and the associated grayscale image, a number of GLCM-based texture features can be derived, such as entropy [15], energy [15], correlation [15], contrast [15], sum of squares (variance) [15],

TABLE I
CLINICAL INFORMATION FOR SUBJECTS IN THE HEALTHY CONTROL (HC) GROUP

Subject #	Age (years)	Height (meters)	Weight (kg)	Gender	Gait Speed (m/sec)	Severity
1	57	1.94	95	F	1.33	0
2	22	1.94	70	M	1.47	0
3	23	1.83	66	F	1.44	0
4	52	1.78	73	F	1.54	0
5	47	1.94	82	F	1.54	0
6	30	1.81	59	F	1.26	0
7	22	1.86	64	F	1.54	0
8	22	1.78	64	F	1.33	0
9	32	1.83	68	F	1.47	0
10	38	1.67	57	F	1.4	0
11	69	1.72	68	F	0.91	0
12	74	1.89	77	M	1.26	0
13	61	1.86	60	F	1.33	0
14	20	1.9	57	F	1.33	0
15	20	1.83	50	F	1.19	0
16	40	1.74	59	F	1.33	0

TABLE II
CLINICAL INFORMATION FOR SUBJECTS IN THE PARKINSON'S DISEASE (PD) GROUP

Subject #	Age (years)	Height (meters)	Weight (kg)	Gender	Gait Speed (m/sec)	Severity
1	77	2.00	86	M	0.98	4
2	44	1.67	54	F	1.26	1.5
3	80	1.81	77	M	0.98	2
4	74	1.72	43	F	0.91	3.5
5	75	1.92	91	M	1.05	2
6	53	2.00	86	M	1.33	2
7	64	1.67	54	F	0.91	4
8	64	1.83	73	M	0.84	4
9	68	1.92	84	M	1.05	1.5
10	60	1.94	74	M	1.19	3
11	74	2.04	100	M	0.5	3
12	57	1.72	65	F	0.98	3
13	79	1.68	59	F	0.84	3
14	57	2.13	84	M	0.98	3
15	76	2.00	96	M	1.19	2.5

TABLE III
CLINICAL INFORMATION FOR SUBJECTS IN THE HUNTINGTON'S DISEASE (HD) GROUP

Subject #	Age (years)	Height (meters)	Weight (kg)	Gender	Gait Speed (m/sec)	Severity
1	42	1.86	72	M	1.68	8
2	41	1.78	58	F	1.05	11
3	66	1.75	63	F	1.05	4
4	47	1.88	64	F	1.4	2
5	36	2.00	85	M	1.82	10
6	41	1.83	59	F	1.54	8
7	71	2.00	75	M	1.05	2
8	53	1.81	56	F	1.26	9
9	54	1.8	90	F	1.26	12
10	47	1.78	102	F	1.05	4
11	33	1.97	84	M	1.26	11
12	47	1.92	75	M	1.19	8
13	40	1.72	48	F	0.56	5
14	36	1.88	97	F	1.4	12
15	34	1.94	88	F	0.56	3
16	70	1.83	93	M	0.56	5
17	29	1.78	76	F	1.19	12
18	54	1.72	53	F	0.98	2
19	59	1.78	58	F	0.98	1
20	33	1.57	45	F	x	9

sum average [15], sum variance [15], sum entropy [15], difference variance [15], difference entropy [15], two information measures of correlation [15], autocorrelation [17], dissimilarity [17], homogeneity [17], cluster prominence [17], cluster shade [17], maximum probability [17], and inverse difference [18].

IV. GAIT-DYNAMICS DATA

The Gait Dynamics in Neuro-Degenerative Disease Database [2], [3], which is publically available (https://www.physionet.org/physiobank/database/gaitndd/), was used in this study. The database consists of the raw data obtained by using force-sensitive resistors, where the output being proportional

TABLE IV
CLINICAL INFORMATION FOR SUBJECTS IN THE AMYOTROPHIC LATERAL SCLEROSIS (ALS) GROUP

Subject #	Age (years)	Height (meters)	Weight (kg)	Gender	Gait Speed (m/sec)	Duration (months)
1	68	1.80	86.18	M	1.302	1
2	63	1.83	83.92	M	1.219	14
3	70	1.57	40.82	F	0.853	13
4	70	1.70	58.97	F	x	54
5	36	1.70	74.39	M	x	5.5
6	43	1.75	68.95	M	0.77	17
7	65	1.73	81.65	M	1.302	9
8	51	1.83	106.6	M	1.085	3
9	50	1.58	61.24	M	0.899	54
10	40	1.70	61.24	F	1.219	14.5
11	39	1.88	83.92	M	1.283	7
12	62	1.78	117.5	M	0.831	12
13	66	1.83	x	M	0.832	34

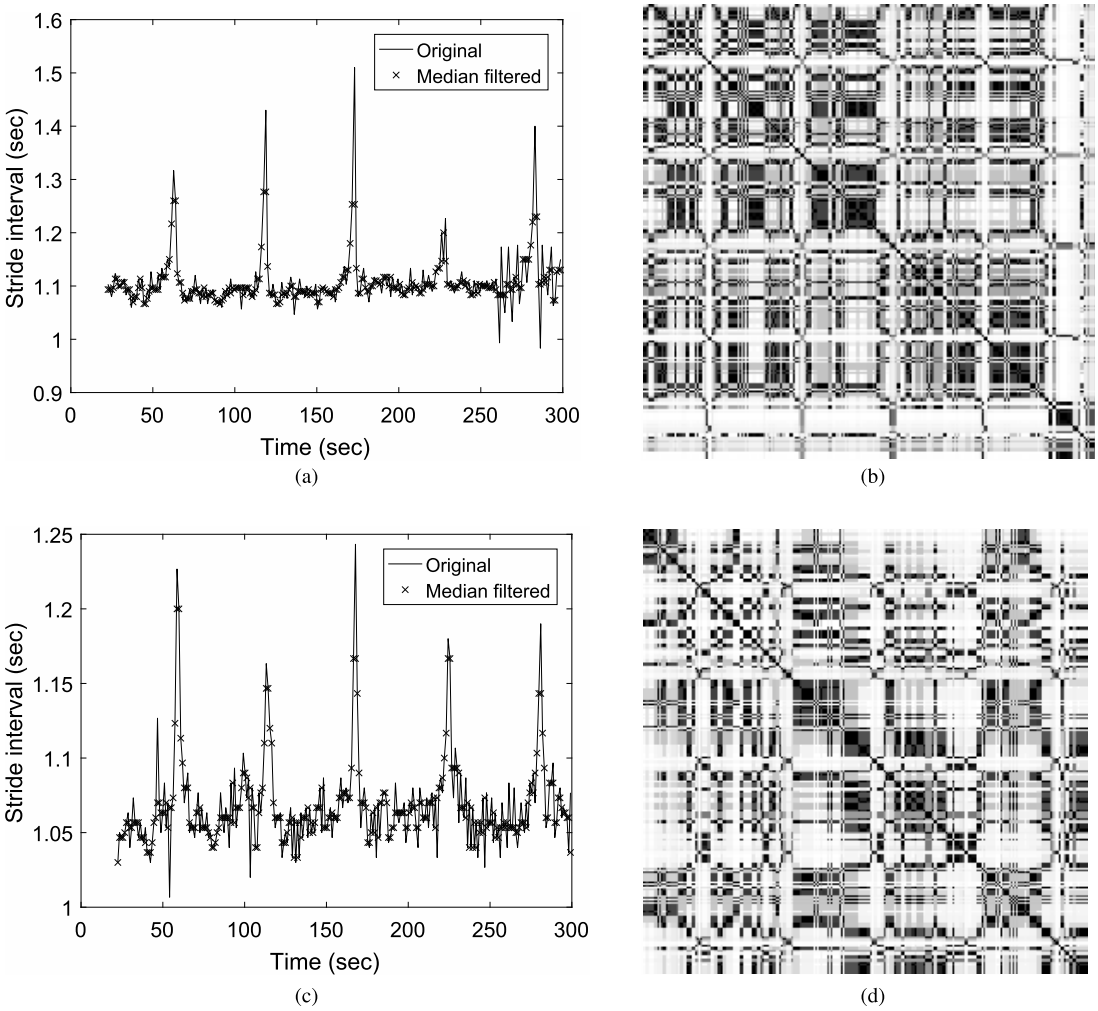

Fig. 1. Gait signals and fuzzy recurrence plots (FRPs) of healthy control (HC) subjects 12 and 14. (a) Gait signal of HC #12. (b) FRP of HC #12. (c) Gait signal of HC #14. (d) FRP of HC #14.

to the force under the foot, of healthy control (HC) subjects and three types of neuro-degenerative disease: Parkinson's disease (PD), Huntington's disease (HD), and amyotrophic lateral sclerosis (ALS). The numbers of control subjects = 16, PD patients = 15, HD patients = 20, and ALS patients = 13. Stride-to-stride measures of footfall contact times were derived from these signals.

Tables I, II, III, and IV show the clinical information for subjects in the HC, PD, HD, and ALS groups, including age, gender, height, weight, walking speed, and a measure of disease severity (PD and HD) or duration (ALS). For the PD patients, the Hoehn and Yahr scale of stages 1 through 5 [19] is used, where a higher scale indicates more advanced disease, and "x" indicates missing. For the HD patients, the total

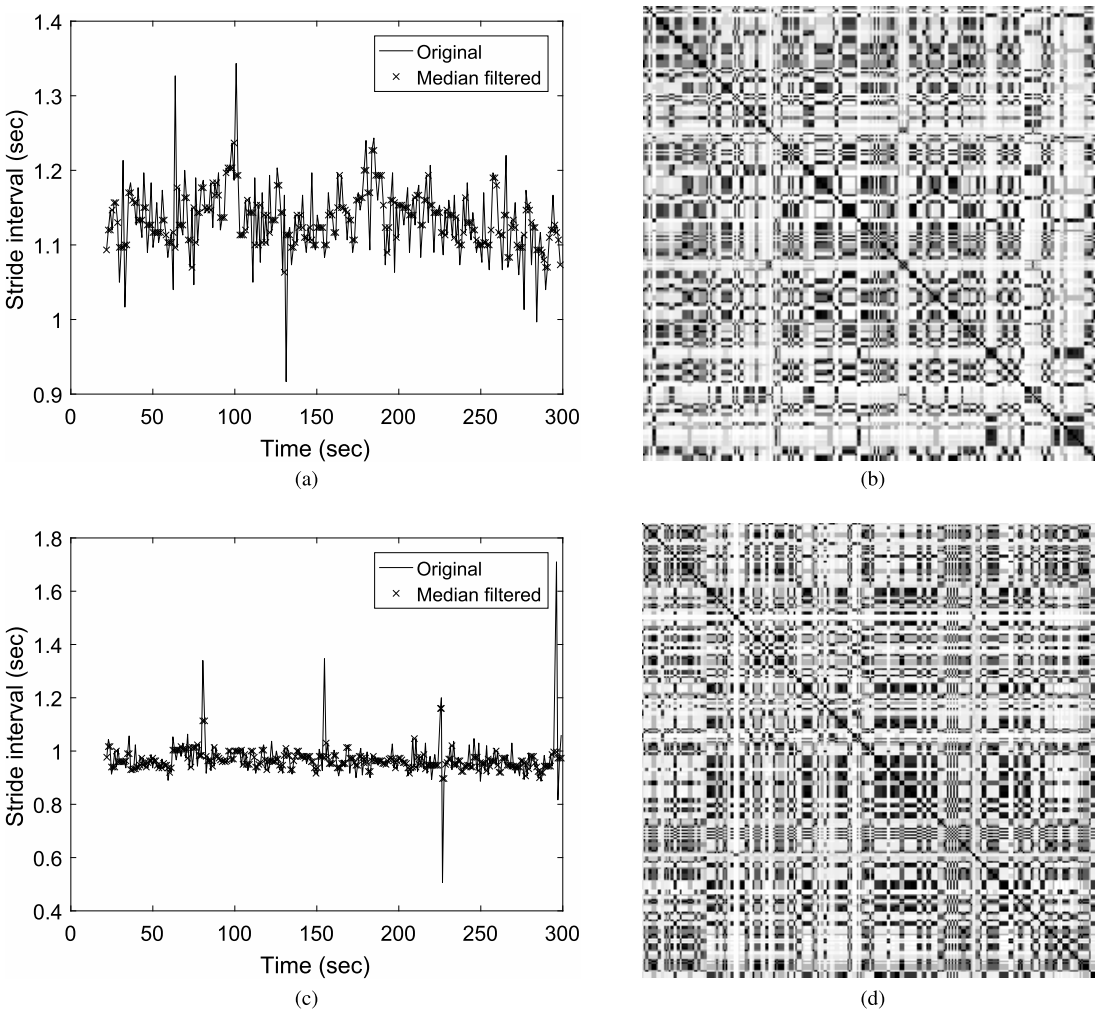

Fig. 2. Gait signals and fuzzy recurrence plots (FRPs) of Parkinson's disease (PD) subjects 1 and 2. (a) Gait signal of PD #1. (b) FRP of PD #1. (c) Gait signal of PD #2. (d) FRP of PD #2.

functional capacity measure is applied, where a lower score indicates more advanced functional impairment. For the ALS patients, the value is the time in months since the diagnosis of the disease. For the control subjects, an indicator of 0 is used.

V. Results and Discussion

The right-foot stride-interval signals of the HC, PPD, HD, and ALS groups were used in this study for constructing FRPs, texture feature extraction, and pattern classification. The parameters for constructing the FRPs were selected as follows: embedding dimension $m = 1$, time delay $\tau = 1$, and the number of clusters $c = 5$, where the maximum number of iterations and the minimum value for improvement (κ) in the objective function between two consecutive iterations of the FCM algorithm were 100 and 0.00001, respectively, and the fuzzy weighting exponent $\omega = 2$. The stride intervals are the durations measured in seconds from the time the foot contacted the ground to the next ground contact of the same foot. The raw signals were smoothed using the third-order one-dimensional median filter. Figures 1, 2, 3, and 4 show the right-foot stride-interval signals and associated fuzzy recurrence plots of two subjects of each of the HC, PD, HD, and ALS groups. The subjects shown in these figures were selected with a purpose to reflect the contrast in age in the HC group (subject 12's age = 74 years, and subject 14's age = 20 years), severity in the PD group (subject 1's severity = 4, and subject 2's severity = 1.5), severity in the HD group (subject 9's severity = 12, and subject 19's severity = 1), and the duration of the disease onset in the ALS group (subject 1's duration = 1 months, and subject 4's duration = 54 months). Given the most contrast of patterns within the individual groups, the FRPs visually exhibit similar textures of the pairs of gait signals in the same groups, and difference in texture patterns of the the FRPs of the pairs of gait signals between the four groups can be observed. The FRPs of the two ALS subjects have the largest number of dark pixels, indicating the most frequent visits of the phase-space states of the systems. This can be explained by the relatively lowest level of fluctuation of the gait signals of the two ALS subjects. The intra-similarity of the FRP texture patterns can be more easily observed in the clusters in diagonal orientations, where the difference is mostly characterized by the image shading, which is expressed in terms of the different fuzzy degrees of occurrence of the phase-space states.

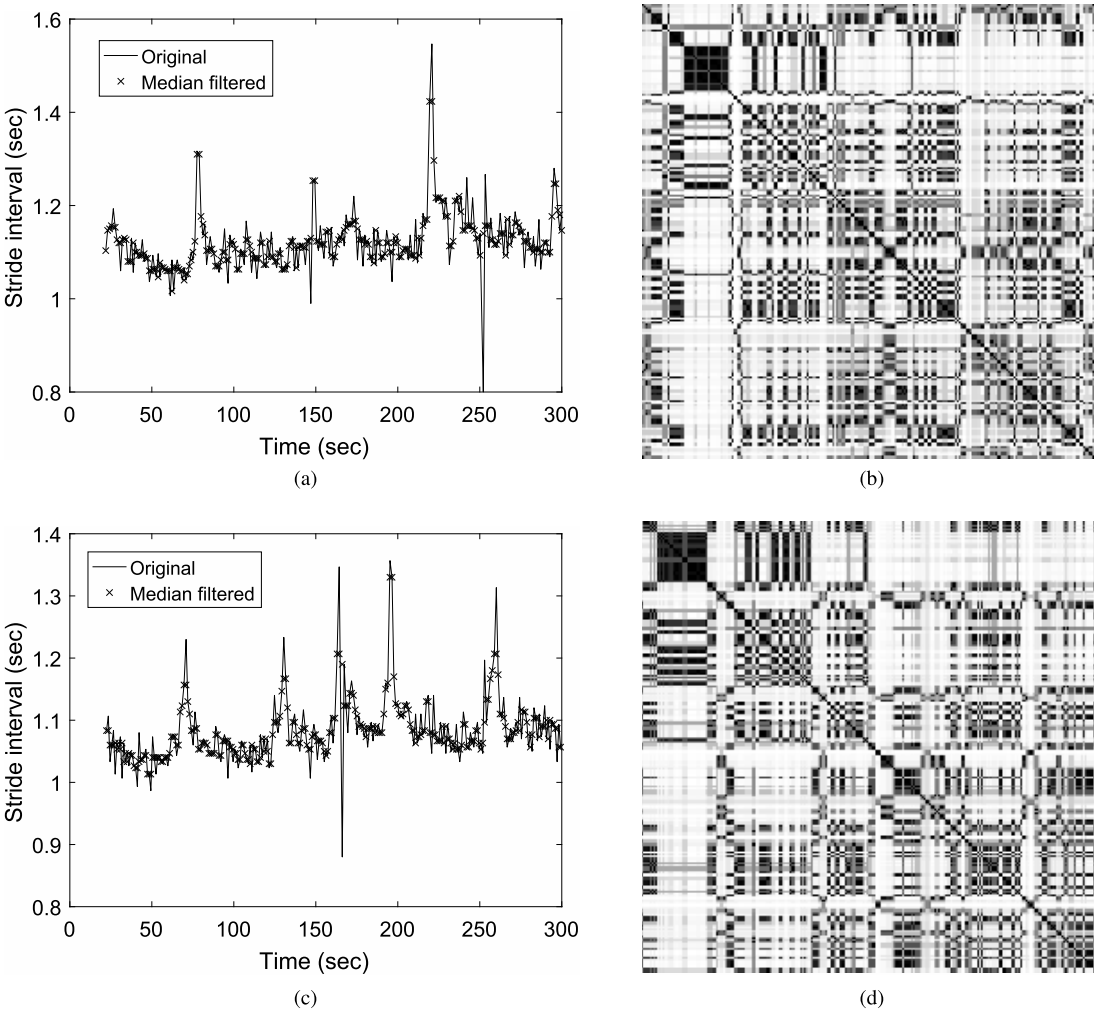

Fig. 3. Gait signals and fuzzy recurrence plots (FRPs) of Huntington's disease (HD) subjects 9 and 19. (a) Gait signal of HD #9. (b) FRP of HD #9. (c) Gait signal of HD #19. (d) FRP of HD #19.

Nineteen GLCM-based features were extracted from the FRPs. The orientation for computing the GLCM is one pixel to the right, which indicates $d = 1$ and $\theta = [0, 1]$. The means and standard deviations of the 19 GLCM-based features are shown in Table V, where T1 = autocorrelation, T2 = cluster prominence, T3 = cluster shade, T4 = contrast, T5 = correlation, T6 = difference entropy, T7 = difference variance, T8 = dissimilarity, T9 = energy, T10 = entropy, T11 = homogeneity, T12 = information measure of correlation 1, T13 = information measure of correlation 2, T14 = inverse difference, T15 = maximum probability, T16 = sum average, T17 = sum entropy, T18 = sum of squares variance, and T19 = sum variance. The six texture features that well distinguish HC from PD, HD, and ALS groups are T1, T2, T3, T11, T17, and T18. Particularly, the cluster shade (T3) is a measure of the skewness of the GLCM and its purpose is to quantify the perceptual concepts of uniformity [20], and cluster prominence (T2) quantifies the variation in grayscale as found in sonographic features between the normal and postradiotherapy parotid glands [21]. The mean values of T14 (inverse difference) of the four groups are the same (0.0008×10^3) but having different standard deviations. The standard deviations of the textures of the HC group are smallest, and the standard deviations of the textures of the PD group are smaller than those of both HD and ALS groups. This is in agreement with the finding that in healthy control subjects, the variance of gait dynamics is relative small in comparison with PD, HD, and ALS subjects [3]. The p-values < 0.000001 were obtained for all texture features, except the p-value of T3 (cluster shade) of the ALS group $= 0.0064$, which demonstrate the statistical significance of the texture features of the four groups.

To differentiate HC subjects from PD, HD, and ALS subjects, the Least Squares Support Vector Machines (LS-SVM) toolbox (LS-SVMlab v1.8) [22], which is publically available (http://www.esat.kuleuven.be/sista/lssvmlab/), was used in this study for the classification task. Using the leave-one-out (LOO) cross-validation, the LS-SVM trained and tested with the GLCM-based features extracted from the FRPs, denoted as FRP (LS-SVM), of the gait signals achieved 100% for the accuracy (ACC), sensitivity (SEN), and specificity (SPE), and 1 (maximum value) for the area under curve (AUC) of the Receiver Operating Characteristic (ROC) curve in all three binary classification cases of HC and PD, HC and HD, and HC and ALS.

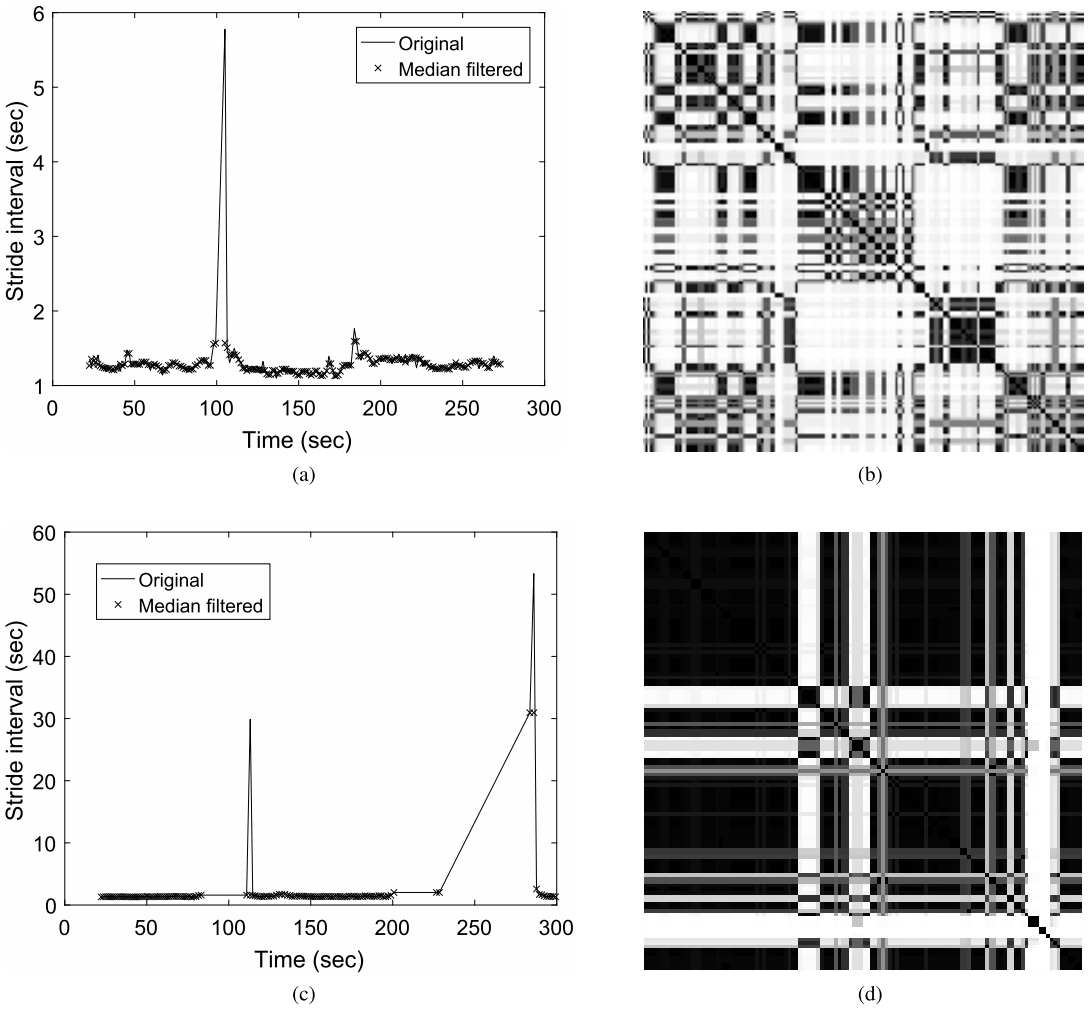

Fig. 4. Gait signals and fuzzy recurrence plots (FRPs) of amyotrophic lateral sclerosis (ALS) subjects 1 and 4. (a) Gait signal of ALS #1. (b) FRP of ALS #1. (c) Gait signal of ALS #4. (d) FRP of ALS #4.

TABLE V

MEANS (μ) AND STANDARD DEVIATIONS (σ) OF GLCM-BASED TEXTURE FEATURES OBTAINED FROM FRPS OF HEALTHY CONTROL (HC), PARKINSON'S DISEASE (PD), HUNTINGTON'S DISEASE (HD), AND AMYOTROPHIC LATERAL SCLEROSIS (ALS) GROUPS

Texture	HC		PD		HD		ALS	
	μ ($\times 10^3$)	σ	μ ($\times 10^3$)	σ	μ ($\times 10^3$)	σ	μ ($\times 10^3$)	σ
T1	0.0410	1.8091	0.0414	3.3251	0.0428	2.2179	0.0390	7.9936
T2	1.0544	83.1435	1.0758	83.3166	1.1147	495.1626	1.2209	281.8654
T3	-0.0831	9.7143	-0.0836	13.4509	-0.0920	40.4738	-0.0617	67.4312
T4	0.0052	0.8822	0.0048	1.1958	0.0052	1.5167	0.0043	1.3465
T5	0.0006	0.0618	0.0006	0.1039	0.0006	0.1308	0.0007	0.1204
T6	0.0012	0.0865	0.0012	0.1025	0.0012	0.2754	0.0011	0.1864
T7	0.0040	0.5978	0.0037	0.7970	0.0040	1.0633	0.0034	0.8417
T8	0.0011	0.1452	0.0010	0.1953	0.0011	0.2900	0.0009	0.2596
T9	0.0002	0.0432	0.0002	0.0395	0.0002	0.0998	0.0002	0.0633
T10	0.0026	0.1792	0.0026	0.1648	0.0025	0.4604	0.0024	0.2652
T11	0.0007	0.0278	0.0008	0.0329	0.0008	0.0626	0.0008	0.0550
T12	-0.0003	0.0401	-0.0003	0.0636	-0.0003	0.1502	-0.0004	0.1003
T13	0.0008	0.0361	0.0008	0.0569	0.0008	0.0503	0.0008	0.0669
T14	0.0008	0.0239	0.0008	0.0286	0.0008	0.0551	0.0008	0.0479
T15	0.0004	0.0516	0.0004	0.0485	0.0005	0.0789	0.0005	0.0888
T16	0.0122	0.3220	0.0122	0.6735	0.0125	0.3087	0.0116	1.8441
T17	0.0021	0.1261	0.0020	0.1172	0.0019	0.3338	0.0020	0.1751
T18	0.0064	0.3393	0.0063	0.6234	0.0062	0.6586	0.0068	1.4324
T19	0.0203	1.1838	0.0203	2.8417	0.0195	3.7464	0.0230	6.1030

Using the same database, the work reported in [4] used both stance and swing intervals to obtain the standard deviations of the probability density functions with the Parzen-window method, and the stride interval, swing interval, and stance interval to extract the signal turn count (STC) parameters to classify HC and PD with the same LS-SVM toolbox.

TABLE VI
COMPARISONS OF RECEIVER OPERATING CHARACTERISTICS AND LOO CROSS-VALIDATION RESULTS FOR CLASSIFICATION OF HC AND PD SUBJECTS, WHERE "x" INDICATES NOT AVAILABLE

Method	SEN (%)	SPE (%)	AUC	ACC (%)
σ & STC (LS-SVM) [4]	x	x	0.952	90.32
RD (HMM) [5]	93.33	87.50	x	90.32
EMD (RF) [9]	x	x	0.865	x
EMD (SLR) [9]	x	x	0.949	x
EMD (MLP) [9]	x	x	0.910	x
EMD (NB) [9]	x	x	0.875	x
EMD (SVM) [9]	x	x	0.906	x
DL [6]	86.67	86.50	x	87.10
FRP (LS-SVM)	100	100	1	100

The AUC and accuracy of this method obtained from the LOO cross-validation using the LS-SVM classifier, denoted as σ & STC (LS-SVM), are 0.952 and 90.32%, respectively. Another report [5] using continuous hidden Markov models of the raw data, denoted as RD (HMM), of the right-foot stride intervals of the same HC and PD subjects to carry out the classification task achieved the same accuracy rate of 90.32% as the σ & STC method, with sensitivity = 93.33% (14/15) and specificity = 87.50% (14/16). The work reported in [6] applied a deterministic learning method, denoted as DL, to extract 4 features based on the information of the average swing, stance and stride intervals, and the fluctuations of the time series, all with both left and right feet. The LOO cross-validation of these features using the DL method obtained for classifying HC and PD is 87.10%, with sensitivity = 86.67% and specificity = 86.50%. Most recently, the empirical mode decomposition (EMD) [9] was used to extract features of 5 gait signals (stride interval, swing interval, stance interval, percentage swing interval, and percentage stance interval) to obtain the Kendall coefficients of concordance and ratios for energy change, which were used for classification by the random forest, denoted as EMD (RF), simple logistic regression, denoted as EMD (SLR), multilayer perceptron, denoted as EMD (MLP), Naive Bayes, denoted as EMD (NB), and support vector machine, denoted as EMD (SVM). The AUCs obtained from the five classifiers EMD (RF), EMD (SLR), EMD (MLP), EMD (NB), and EMD (SVM) are 0.865, 0.949, 0.910, 0.875, and 0.906, respectively. Those results are shown in Table IV. The σ & STC features [4] were also used to differentiate HC from PD subjects using the linear discriminant analysis (LDA), where the LOO cross-validation = 67.74%. The LOO cross-validation of the FRP using LDA is 77.42%. Table VII shows these comparative results for the classification of the HC and PD subjects.

For the LOO cross-validation of the HC and HD groups, the DL method [6] provided the accuracy = 83.33%, sensitivity = 85.00%, and specificity = 81.25%. The AUCs obtained from the five classifiers EMD (RF), EMD (SLR), EMD (MLP), EMD (NB), and EMD (SVM) [9] are 0.885, 0.843, 0.878, 0.898, and 0.900, respectively. Table VIII shows the comparative classification results obtained from the proposed FRP and other methods (DL and EMD).

For the LOO cross-validation of the HC and ALS groups, the DL method [6] provided the accuracy = 89.66%, sensitivity = 92.31%, and specificity = 87.50%. The AUCs obtained from the five classifiers EMD (RF), EMD (SLR), EMD (MLP), EMD (NB), and EMD (SVM) [9] are 0.900, 0.859, 0.934, 0.891, and 0.906, respectively. Table IX shows the comparative classification results obtained from the proposed FRP and other methods (DL and EMD).

TABLE VII
COMPARISONS OF LOO CROSS-VALIDATION RESULTS FROM LDA-BASED CLASSIFICATION OF HC AND PD SUBJECTS

Method	ACC (%)
σ & STC [4]	67.74
FRP	77.42

TABLE VIII
COMPARISONS OF RECEIVER OPERATING CHARACTERISTICS AND LOO CROSS-VALIDATION FOR CLASSIFICATION OF HC AND HD SUBJECTS, WHERE "x" INDICATES NOT AVAILABLE

Method	SEN (%)	SPE (%)	AUC	ACC (%)
EMD (RF) [9]	x	x	0.885	z
EMD (SLR) [9]	x	x	0.843	x
EMD (MLP) [9]	x	x	0.878	x
EMD (NB) [9]	x	x	0.898	x
EMD (SVM) [9]	x	x	0.900	x
DL [6]	85.00	81.25	x	83.33
FRP (LS-SVM)	100	100	1	100

TABLE IX
COMPARISONS OF RECEIVER OPERATING CHARACTERISTICS AND LOO CROSS-VALIDATION FOR CLASSIFICATION OF HC AND ALS SUBJECTS, WHERE "x" INDICATES NOT AVAILABLE

Method	SEN (%)	SPE (%)	AUC	ACC (%)
EMD (RF) [9]	x	x	0.900	x
EMD (SLR) [9]	x	x	0.859	x
EMD (MLP) [9]	x	x	0.934	x
EMD (NB) [9]	x	x	0.891	x
EMD (SVM) [9]	x	x	0.906	x
DL [6]	92.31	87.50	x	89.66
FRP (LS-SVM)	100	100	1	100

In summary, Tables VI, VII, VIII, and IX indicate that the proposed method provide the best results over several other methods for classifying patterns of gait dynamics between HC subjects and PD, HD, and ALS patients.

VI. CONCLUSION

A procedure for transforming physiological time series into images of rich texture using the fuzzy recurrence plot method has been presented and applied for characterization and classification of gait dynamics of healthy control and the three neuro-degenerative diseases. The fuzzy recurrence plots can be useful for visualizing textural patterns of physiological signals. The extraction of texture features from fuzzy recurrence plots using the gray-level co-occurrence matrix method fits well into the underlying mechanism for capturing information content from data carried out by the two methods. The combination of the GLCM-based texture features extracted from the FRPs of the time series of the right-foot stride intervals, and the LS-SVM classifier is promising for differentiating healthy control subjects from patients with neuro-degenerative disease.

As suggested on the database website, the study of finding if the dynamics of the sub-phases of the stride (stance and swing intervals)) is identical to that of the stride itself is worth pursuing by using the recurrence quantification analysis [12] of the fuzzy recurrence plots at different cut-off fuzzy membership grades. This study may also discover if stride nonlinear dynamics changes with various diseases.

REFERENCES

[1] D. H. Lowenstein, J. B. Martin, and S. L. Hauser, "Approach to the patient with neurologic disease," in *Harrison's Principles of Internal Medicine*, D. L. Longo *et al.* Eds., 18th ed. New York, NY, USA: McGraw-Hill, 2012, ch. 367.

[2] J. M. Hausdorff *et al.*, "Altered fractal dynamics of gait: Reduced stride-interval correlations with aging and Huntington's disease," *J. Appl. Physiol.*, vol. 82, no. 1, pp. 262–269, 1997.

[3] J. M. Hausdorff, A. Lertratanakul, M. E. Cudkowicz, A. L. Peterson, D. Kaliton, and A. L. Goldberger, "Dynamic markers of altered gait rhythm in amyotrophic lateral sclerosis," *J. Appl. Physiol.*, vol. 88, no. 6, pp. 2045–2053, 2000.

[4] Y. Wu and S. Krishnan, "Statistical analysis of gait rhythm in patients with Parkinson's disease," *IEEE Trans. Neural Syst. Rehabil. Eng.*, vol. 18, no. 2, pp. 150–158, Apr. 2010.

[5] A. Khorasani and M. R. Daliri, "HMM for classification of Parkinson's disease based on the raw gait data," *J. Med. Syst.*, vol. 38, p. 147, Dec. 2014.

[6] W. Zeng and C. Wang, "Classification of neurodegenerative diseases using gait dynamics via deterministic learning," *Inf. Sci.*, vol. 317, pp. 246–258, Oct. 2015.

[7] W. Zeng, F. Liu, Q. Wang, Y. Wang, L. Ma, and Y. Zhang, "Parkinson's disease classification using gait analysis via deterministic learning," *Neurosci. Lett.*, vol. 633, pp. 268–278, Oct. 2016.

[8] C. Kamath and Z. Jin, "Analysis of altered complexity of gait dynamics with aging and Parkinson's disease using ternary Lempel–Ziv complexity," *Cogent Eng.*, vol. 3, no. 1, 2016, Art. no. 1177924.

[9] P. Ren *et al.*, "Gait rhythm fluctuation analysis for neurodegenerative diseases by empirical mode decomposition," *IEEE Trans. Biomed. Eng.*, vol. 64, no. 1, pp. 52–60, Jan. 2017.

[10] T. D. Pham, "Fuzzy recurrence plots," *Europhys. Lett.*, vol. 116, no. 5, p. 50008, 2016.

[11] J.-P. Eckmann, S. O. Kamphorst, and D. Ruelle, "Recurrence plots of dynamical systems," *Europhys. Lett.*, vol. 5, no. 9, pp. 973–977, 1987.

[12] N. Marwan, M. C. Romano, M. Thiel, and J. Kurths, "Recurrence plots for the analysis of complex systems," *Phys. Rep.*, vol. 438, nos. 5–6, pp. 237–329, Jan. 2007.

[13] L. A. Zadeh, "Similarity relations and fuzzy orderings," *Inf. Sci.*, vol. 3, no. 2, pp. 177–200, Apr. 1971.

[14] J.C. Bezdek, *Pattern Recognition With Fuzzy Objective Function Algorithms*. New York, NY, USA: Plenum, 1981.

[15] R. M. Haralick, K. Shanmugam, and I. Dinstein, "Textural features for image classification," *IEEE Trans. Syst., Man, Cybern.*, vol. SMC-3, no. 6, pp. 610–621, Nov. 1973.

[16] M. Petrou and P. G. Sevilla, *Image Processing: Dealing With Texture*. Chichester, U.K.: Wiley, 2006.

[17] L. K. Soh and C. Tsatsoulis, "Texture analysis of SAR sea ice imagery using gray level co-occurrence matrices," *IEEE Trans. Geosci. Remote Sens.*, vol. 37, no. 2, pp. 780–795, Mar. 1999.

[18] D. A. Clausi, "An analysis of co-occurrence texture statistics as a function of grey level quantization," *Can. J. Remote Sens.*, vol. 28, no. 1, pp. 45–62, 2002.

[19] M. Hoehn and M. Yahr, "Parkinsonism: Onset, progression and mortality," *Neurology*, vol. 17, no. 5, pp. 427–442, 1967.

[20] M. Unser, "Sum and difference histograms for texture classification," *IEEE Trans. Pattern Anal. Mach. Intell.*, vol. PAMI-8, no. 1, pp. 118–125, Jan. 1986.

[21] X. Yang *et al.*, "Ultrasound GLCM texture analysis of radiation-induced parotid-gland injury in head-and-neck cancer radiotherapy: An *in vivo* study of late toxicity," *Med. Phys.*, vol. 39, no. 9, pp. 5732–5739, Sep. 2012.

[22] J. A. K. Suykens, T. Van Gestel, J. De Brabanter, B. De Moor, and J. Vandewalle, *Least Squares Support Vector Machines*. Singapore: World Scientific, 2002.